PHYSICAL REVIEW B **83**, 220102(R) (2011)

Thermodynamic identification of tungsten borides

Yongcheng Liang,[1,2] Xun Yuan,[1] and Wenqing Zhang[1]

[1]*State Key Laboratory of High Performance Ceramics and Superfine Microstructures, Shanghai Institute of Ceramics, Chinese Academy of Sciences, Shanghai 200050, China*

[2]*Institute of Ocean Engineering and College of Engineering Science and Technology, Shanghai Ocean University, Shanghai 201306, China*

(Received 22 April 2011; revised manuscript received 29 May 2011; published 21 June 2011)

Combining first-principles calculations with thermodynamics, we evaluate the structure stability of the boron-tungsten system (WB_x), which is a promising superhard material. The highest boride of tungsten, previously denoted WB_4 with a three-dimensional boron network, is identified as WB_3 with two-dimensional boron nets. Furthermore, it is revealed that the mechanical properties of WB_x correlate with their formation energies, which justifies the thermodynamic considerations in the design of intrinsically hard materials.

DOI: 10.1103/PhysRevB.83.220102 PACS number(s): 61.50.Ah, 61.50.Ks, 62.20.−x

Transition metal borides have attracted much attention for a long time since they are refractory, chemically inert, and hard substances with high thermal and electrical conductivity.[1] Nowadays, several experimental researches (OsB_2, ReB_2, $RhB_{1.1}$, and $IrB_{1.35}$) (Refs. 2–4) have reinvigorated the fundamental question of whether transition metal borides become intrinsically superhard materials. However, common issues on the ambiguity of crystal structures still remain in transition metal borides. Because of the large mass difference between transition metal atoms and boron atoms, only the positions of the metal atoms can be directly determined by x-ray diffraction, but the arrangements of the boron atoms are speculated from space considerations, assuming that boron atoms occupy the largest holes of the metal lattice. Moreover, transition metal borides have rich phase diagrams and many phases coexist. Chemical analysis may not distinguish between free and chemically bound boron. These technological difficulties contribute to the uncertainty of the boron architecture. It is therefore highly desirable to develop a theoretical method to identify the exact composition and structure and, in particular, to provide the essential guidance in the design of superhard materials.

Recently, WB_x has raised many expectations for future superhard materials. The Vickers hardness of WB_2 was reported to be quite high with a value of 43.8–47.4 GPa (Ref. 5). The micro-indentation test has revealed that the claimed WB_4 has extremely high hardness (Vickers hardness 46.2 GPa) (Ref. 6). Compared to boron-poor borides, boron-rich borides not only reduce the weight and cost of materials, but also increase covalent bonding, and thus the particular interest lies in WB_4. Instead, the agreements are far from complete on the composition and structure of WB_x. Recent work[7] confirmed that the earliest established W_2B_5 (Ref. 8) should be W_2B_4. The AlB_2-type WB_2 has been reported as the experimental ground state,[9] but theoretical calculations[5,10] recently showed that it is actually a high-pressure phase. However, the ReB_2 type becomes the ground state phase. For WB_4, it seems as if the experimental and theoretical studies[6,11] reached the consensus that the three-dimensional boron network composed of an in-plane honeycomb B sublattice and an out-of-plane B_2 dimer is responsible for its high hardness. Nevertheless, it is a bit surprising that such a hard material has so low a shear modulus (103.6–129.1 GPa) (Ref. 11).

In this Rapid Communication, a thermodynamic approach combining first-principles calculations with chemical potentials is applied to investigate reasonable structures of WB_x at pressures up to 80 GPa. Seventeen candidate structures were chosen for WB_x, namely, tetragonal W_2B, tetragonal WB, orthorhombic CrB and FeB, hexagonal PtB and OsB, hexagonal ReB_2, orthorhombic OsB_2, rhombohedral MoB_2, hexagonal WB_2 and AlB_2, hexagonal W_2B_5, hexagonal MoB_3, orthorhombic CrB_4, monoclinic MnB_4, hexagonal WB_4, and tetragonal ThB_4 type.[12,13] We have identified that the long assumed WB_4 is, in fact, WB_3 with two-dimensional boron nets, which reformulates the concept of the three-dimensional boron network responsible for its high hardness. Furthermore, our results indicate that the ReB_2-type structure, which is corroborated to be the ground state for WB_2, transforms into the MoB_2 type above 9.2 GPa.

The bridge between first-principles calculations and thermodynamics was established to analyze the structural stability of complex materials that can involve intrinsic nonstoichiometries of the chemical compositions.[14] We utilize this theory to explore the stable structures for stoichiometric borides. For simplicity, only the binary system WB_x is considered. Based on the chemical reaction $W + xB = WB_x$, our strategy is to seek the state with the lowest Gibbs energy G_S: $G_S = G_0 - \mu_W - x\mu_B$. Here G_0 means the free energy of an ensemble WB_x, and μ_W (μ_B) is the chemical potential of the component tungsten (boron) at a specified thermodynamic environment with temperature T and pressure p. Although chemical potentials can be defined for defects and defect complexes,[14] they are not included in the above equation since we focus on the stoichiometric phases of WB_x. For an ensemble WB_x, its free energy G_0 can be written as $G_0 = E(T,p) + pV - TS$, where $E(T,p)$ and S denote its internal energy and entropy, respectively. It is well known that temperature T and pressure p are thermodynamically equivalent. Particularly, the contribution of the term TS to the free energy G_0 is normally weak for other systems[15,16] at room temperature. Thus we only consider the free energy G_0 of an ensemble WB_x at the zero temperature: $G_0 = E(0\mathrm{K},p) + pV$. For clarity, the first-principles effective chemical potential difference is defined as $\Delta\mu_i = \mu_i - \mu_i^0(0\mathrm{K},p)$, where $\mu_i^0(0\mathrm{K},p) = E_i(0\mathrm{K},p) + pV_i$ (i = W or B) is the chemical potential of the body-centered cubic tungsten or alpha rhombohedral boron at the temperature

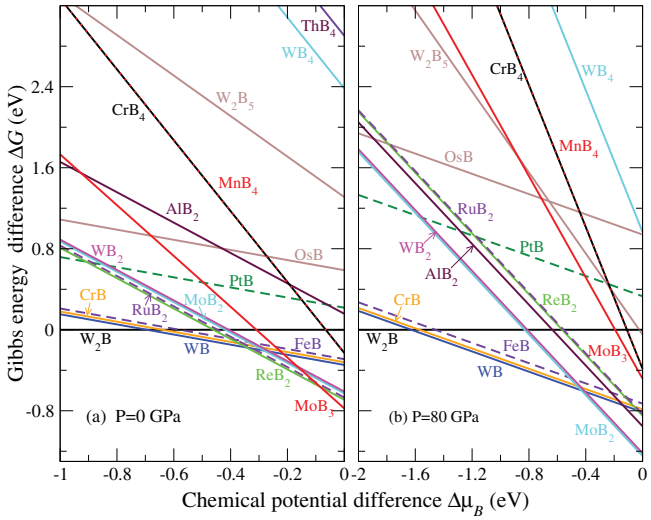

FIG. 1. (Color online) The stabilities of various WB_x relative to W_2B as a function of the chemical potential difference obtained by first-principles calculations at (a) $p = 0$ GPa and (b) $p = 80$ GPa (b).

of $T = 0$ K and the pressure of p. Therefore, the lowest Gibbs energy is rewritten as $G_S = \Delta H - \Delta\mu_W - x\Delta\mu_B$. Here ΔH is the formation enthalpy $\Delta H = E(0K, p) + pV - \mu^0_W(0K, p) - x\mu^0_B(0K, p)$ of WB_x at the temperature of $T = 0$ K and the pressure of p. The quantities $E(0K, p)$ and $\mu^0_i(0K, p)$ are determined by performing density functional calculations within the generalized gradient approximation (GGA).[17] We use the VASP code that implements the projector augmented wave (PAW) method.[18] In reality, this method can be generalized to polynary systems of transition metal borides, carbides, and nitrides. Especially, it takes into account the phase competition of diverse compositions because of the inclusion of the chemical potentials of the constituents.

Figure 1 presents Gibbs energy differences of various candidate WB_x relative to W_2B as a function of the chemical potential difference $\Delta\mu_B$ at pressures of 0 and 80 GPa. In good agreement with experimental observations[8,19] we find that W_2B and WB are thermodynamically stable at zero and high pressure, while the PtB and OsBtype WB are unstable because of their high relative Gibbs energies. The CrB- and FeB-type WB are energetically very close to the WB structure, and thus they may be high-temperature phases. It can be seen that W_2B_5 cannot exist at zero and high pressures, but the similar structure WB_2 is far more favorable in Gibbs energy, which supports the recent theoretical and experimental conclusions[7,10] that W_2B_5 should be WB_2. These reproduced results substantiate the validity of our thermodynamic considerations from the viewpoint of chemical potentials.

Unexpectedly, the MoB_3-type WB_3 has the lowest Gibbs energy among the 17 candidate structures under the boron-rich condition and should be thermodynamically stable [Fig. 1(a)]. However, the highest boride of tungsten WB_4 is found to be highly unstable because of its high relative Gibbs energy. The claimed WB_4 was originally synthesized in 1961,[20] and confirmed by several experiments.[21,22] Moreover, its high hardness inspired recent experimental and theoretical studies.[6,10] Surprisingly, our conclusion on its instability completely conflicts with these.[6,10,20–22] For the AlB_2-type WB_2, it is unlikely that it occurs at ambient condition, which is at odds with the experimental report of Woods *et al.*[9]

At $p = 0$ GPa, the Gibbs energy differences of the ReB_2-, RuB_2-, MoB_2-type WB_2 and WB_2 phases are within the range of 0.1 eV. Among the four phases, the ReB_2 type has the lowest Gibbs energy as the ground state for WB_2 [Fig. 1(a)]. At $p = 80$ GPa, the MoB_2 type becomes more stable than the ReB_2 type, and the MoB_3-type WB_3 becomes thermodynamically unstable [Fig. 1(b)]. To reveal the pressure effect on the stability for five structures of WB_2, we calculate their enthalpies with the range of 0–80 GPa. As shown in Fig. 2, there are crossings between competing structures signifying phase transitions under pressure. We can see that a structural transformation from ReB_2 type to MoB_2 type takes place at $p = 9.2$ GPa. Although the ReB_2 type may transform to the AlB_2 type at $p = 65$ GPa, this latter type has a higher enthalpy than the MoB_2 type. Hence, the AlB_2 type should not be the high-pressure phase for WB_2 below 100 GPa, in contrast with recent calculations.[5,10] As shown in Fig. 1, the boron-rich phases (the CrB_4-, MnB_4-, and ThB_4-type WB_4) have higher Gibbs energies than the boron-poor phases at zero and high pressure, signifying that it is not easy to prepare more boron-rich WB_x ($x > 3$) experimentally.

To solve the contradictions between our and the experimental results on WB_4, further structural analyses are required. In the WB_4 structure (top left inset of Fig. 3), there are four formula units per unit cell with W at $2c$ (1/3, 2/3, 1/4) and $2b$ (0, 0, 1/4) and B at $12i$ (x, 0, 0) with $x = 1/3$ and $4f$ (1/3, 2/3, z) with $z = 0.615$, labeled as W1, W2, B1, and B2, respectively.[21] The B2-B2 distance (1.716 Å) is shorter than that of any known WB_x phases except W_2B_5 (1.72 Å). However, recent studies[7,10] and our results confirm that W_2B_5 is W_2B_4, and such a short B-B distance is improbable. We attempt to substitute vacancies for B2 atoms and calculate the formation energy by $\Delta E = E(WB_x) - E(W) - xE(B)$. The formation energy of unit cell W_4B_{16-y} in the WB_4 structure as a function of vacancy number y is showed in Fig. 3. To our surprise, the formation energy sharply decreases from 1.976 to -1.156 eV/WB_x as the vacancy number y increases from 0 to 4, which confirms that the B2 atoms are unfavorable to the stability. At $y = 4$, corresponding to no occurrence of B2 atoms, the structure of WB_3 is isostructural with MoB_3. As a matter of fact, W_2B and WB are isomorphic with Mo_2B and MoB, respectively.

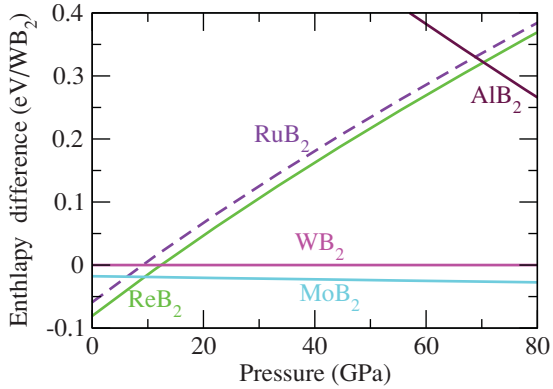

FIG. 2. (Color online) Enthalpy differences of different structures relative to WB_2 as a function of pressure.

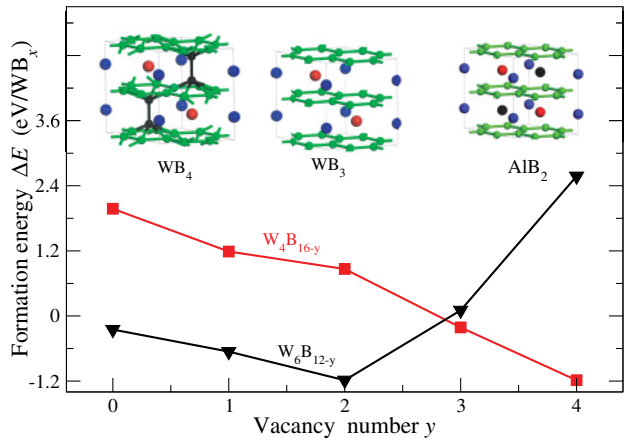

FIG. 3. (Color online) Formation energies for WB_4 and the AlB_2-type WB_2 as a function of the vacancy number. The crystal structures of WB_4, WB_3, and the AlB_2-type WB_2 are inset. In the WB_4 structure, large red, large blue, small green, and small black spheres represent W1, W2, B1, and B2, respectively.

Although MoB_2 and WB_2 have slightly different structures at ambient condition, the MoB_2-type WB_2 becomes more stable than WB_2 above $p = 9.2$ GPa. The analogous nominal MoB_4 was investigated using powder diffractometry in conjunction with the electron microprobe and chemical analysis.[23] There is no experimental evidence that the B2 atoms exist and its correct crystallographic formula is $Mo_{1-x}B_3$. However, due to the heavy W atoms, nominal WB_4 offers considerably bad experimental conditions to restrict the accuracy. Hence, the overall trend of their isomorphism is unmistakable, and we rationally believe that the claimed WB_4 should be WB_3 isostructural with stoichiometric MoB_3. In contrast to the three-dimensional boron network of WB_4, WB_3 is stacked by the two-dimensional boron nets and W layers (top middle inset to Fig. 3).

The WB_3 structure is closely related to the AlB_2 structure, which consists of close packed layers of W atoms located directly above one another with B atoms in the interstices (top right inset to Fig. 3). Hence, the WB_3 phase can be derived from the AlB_2-type WB_2 by replacing one-third of the W atoms with vacancy systematically so that the remaining W atoms form layers of open hexagons with alternate layers displaced by one atom. We regularly substitute vacancies for W atoms of a supercell of $W_{6-y}B_{12}$ in the AlB_2 structure, and calculate their formation energies. It is found from Fig. 3 that the AlB_2-type $W_{6-y}B_{12}$ has the lowest formation energy at $y = 2$. This case corresponds to WB_3. Combined with the thermodynamic instability of the AlB_2-type WB_2 discussed above, we provide direct evidence that the experimental assumed AlB_2-type WB_2 (Ref. 9) is, in fact, the WB_3 phase.

The conclusion that the claimed WB_4 and the AlB_2-type WB_2 are WB_3 are supported by our calculated crystal parameters. The measured lattice constants and volume ($a_0 = 5.159$ Å, $c_0 = 6.332$ Å, $V_0 = 36.99$ Å^3) for WB_4 (Ref. 6) are in very good agreement with the values ($a_0 = 5.209$ Å, $c_0 = 6.312$ Å, $V_0 = 36.97$ Å^3) we calculated for WB_3. In contrast, the calculated results for WB_4 ($a_0 = 5.362$ Å, $c_0 = 6.452$ Å, $V_0 = 40.16$ Å^3) are much larger. For the AlB_2-type WB_2, the experimental lattice constants ($a_0 = 3.02$ Å, $c_0 = 3.05$ Å) of the AlB_2 symmetry[9] are well compatible with our values ($a_0/\sqrt{3} = 3.01$ Å, $c_0/2 = 3.156$ Å) of WB_3. We relax WB_2 restricted to the AlB_2 symmetry. The results show that the c axis (10.2% larger than the experimental value) becomes much longer due to the "extra" W atoms that want to "come off" from their initial positions.

The thermodynamic stability will most probably be reflected in the variation of mechanical properties owing to the correlation that normally exists between two effects. The mechanical properties (bulk modulus, elastic constants, shear modulus, Young's modulus, and Poisson's ratio) are obtained through our previous methods.[24] Figure 4 shows the trends of formation energy, bulk modulus, and shear modulus with the increase of boron content for the 17 structures of WB_x. It is observed that the shear modulus increases with the decrease of the formation energy. Among the phases of the same composition, the phase with the lowest formation energy has the largest shear modulus. However, the bulk modulus has little direct connection with its formation energy. As we know, the formation energy is closely associated with the bonding nature. This explains why the shear modulus is a significantly better qualitative predictor of hardness than the bulk modulus. Therefore, a thermodynamic consideration of stability is warranted for the design of superhard materials.

The correlations between the formation energy and mechanical properties are strongly embodied in the WB_4 and WB_3 phases. Although the bulk moduli of WB_4 (297 GPa) and WB_3 (291 GPa) are in accordance with the experimental result (304 GPa) (Ref. 6), the shear modulus of WB_4 (102 GPa) is only 40% that of WB_3 (252 GPa), even smaller than that of W (150 GPa). According to the linear correlation that exists between the shear modulus and the Vickers hardness for many of the known hard materials,[25] we estimate that WB_3 has a

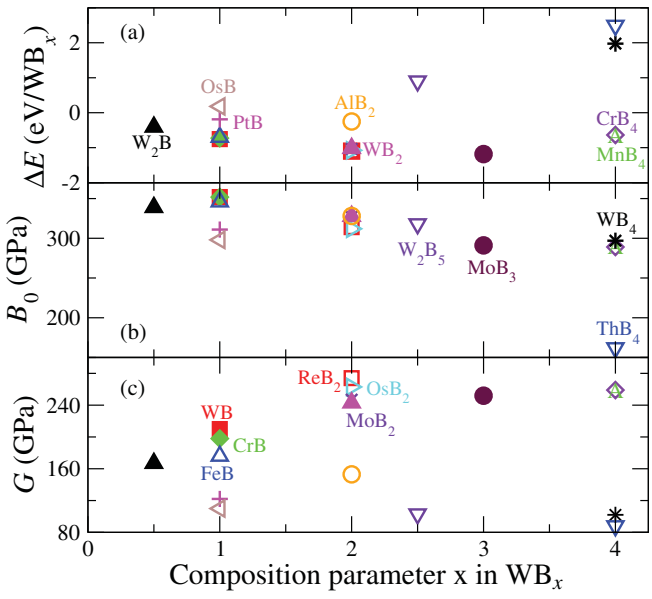

FIG. 4. (Color online) (a) Formation energies, (b) bulk moduli, and (c) shear moduli for various WB_x versus the boron composition parameter x. In (a), (b), and (c) the same symbol denotes the same phase.

Vickers hardness of 42 GPa, consistent with the experimental value of 46.2 GPa (Ref. 6). On the contrary, the estimated hardness of WB_4 (15 GPa) largely deviates from the experimental result. The Poisson's ratio of WB_3 is 0.168, typical for covalent materials such as cBN (0.124) and ReB_2 (0.171) (Ref. 26), while that of WB_4 is 0.348, even larger than that of W (0.293). In addition, the Young's modulus and elastic constants of WB_3 ($E = 588$ GPa, $C_{11} = 656$ GPa, $C_{33} = 479$ GPa, $C_{44} = 277$ GPa) are superior to those of WB_4 ($E = 274$ GPa, $C_{11} = 399$ GPa, $C_{33} = 444$ GPa, $C_{44} = 154$ GPa). The sharp contrasts of their mechanical properties are interrelated with their formation energies. Hence our calculated thermodynamic and mechanical properties provide incontrovertible evidence that the claimed WB_4 is the MoB_3-type WB_3.

As we can see from Fig. 4, the boron-poor phases (W_2B, WB, CrB, and FeB type) have a larger bulk modulus (above 346 GPa), but smaller shear modulus (below 210 GPa), indicating that they are ultra-incompressible but not superhard candidates. The boron-rich phases (ReB_2, WB_3, CrB_4, and MnB_4 type) have a larger shear modulus (above 252 GPa) and thus they are potentially superhard materials. In particular, the CrB_4- and MnB_4-type WB_4 with three-dimensional boron networks have negative formation energies. Moreover, our calculated elastic constants confirm that they are mechanically stable. However, the above analysis shows that the CrB_4- and MnB_4-type WB_4 are thermodynamically unstable. These results point out that only the negative formation energy is not enough for the thermodynamic stability of a phase and the thermodynamic consideration from the viewpoint of chemical potentials is necessary in the design of intrinsically superhard transition metal borides, carbides, and nitrides.

In summary, we present a comprehensive thermodynamic method to assess the phase stability of transition metal borides. The application to WB_x proves that the long regarded WB_4- and AlB_2-type WB_2 are actually WB_3. Furthermore, the ReB_2-type WB_2 is corroborated as the ground state for WB_2 and transforms to the MoB_2 type at $p = 9.2$ GPa. Interestingly, the correlation between the thermodynamic stabilities and mechanical properties for WB_x is clarified to underline the importance of the thermodynamic consideration of stability in the design of superhard materials.

This research was supported by the NSFC (No. 51072213), the Local Colleges Faculty Construction of Shanghai MSTC (No. 08210511900), the Innovation Program of Shanghai MEC (No. 11ZZ147), and the Postdoctoral Foundation of China (No. 20090450738) and Shanghai (No. 10R21416700).

[1] J. B. Levine, S. H. Tolbert, and R. B. Kaner, Adv. Funct. Mater. **19**, 3519 (2009).
[2] R. W. Cumberland, M. B. Weinberger, J. J. Gilman, S. M. Clark, S. H. Tolbert, and R. B. Kaner, J. Am. Chem. Soc. **127**, 7264 (2005).
[3] H. Y. Chung, M. B. Weinberger, J. B. Levine, A. Kavner, J. M. Yang, S. H. Tolbert, and R. B. Kaner, Science **316**, 436 (2007).
[4] J. V. Rau and A. Latini, Chem. Mater. **21**, 1407 (2009).
[5] X. Q. Chen, C. L. Fu, M. Krcmar, and G. S. Painter, Phys. Rev. Lett. **100**, 196403 (2008).
[6] Q. Gu, G. Krauss, and W. Steurer, Adv. Mater. **20**, 3620 (2008).
[7] M. Frotscher, W. Klein, J. Bauer *et al.*, Z. Anorg. Allg. Chem. **633**, 2626 (2007).
[8] R. Kiessing, Acta Chem. Scand. **1**, 893 (1947).
[9] H. P. Woods, F. E. Wawner, and B. G. Fox, Science **151**, 75 (1966).
[10] E. Zhao, J. Meng, Y. Ma, and Z. Wu, Phys. Chem. Chem. Phys. **12**, 13158 (2010).
[11] M. Wang, Y. Li, T. Cui, Y. Ma, and G. Zou, Appl. Phys. Lett. **93**, 101905 (2008).
[12] R. Kiessing, Acta Chem. Scand. **4**, 209 (1950).
[13] T. Lundstrom, Arkiv. Kemi. **31**, 227 (1969).
[14] W. Zhang, J. R. Smith, and X.-G. Wang, Phys. Rev. B **70**, 024103 (2004).
[15] W. Zhang, J. R. Smith, and A. G. Evans, Acta Mater. **50**, 3803 (2002).
[16] K. E. Spear and P. K. Liao, Bull. Alloy Phase Diagrams **9**, 457 (1988).
[17] J. P. Perdew, K. Burke, and M. Ernzerhof, Phys. Rev. Lett. **77**, 3865 (1996).
[18] G. Kresse and J. Furthmuller, Phys. Rev. B **54**, 11169 (1996).
[19] B. Post and F. Glaser, J. Chem. Phys. **20**, 1050 (1952).
[20] A. Chretien and J. Helgorsky, C. R. Acad. Sci. Paris **252**, 742 (1961).
[21] P. A. Romans and M. P. Krug, Acta Cryst. **20**, 313 (1966).
[22] T. Lundstrom, Arkiv. Kemi. **30**, 115 (1968).
[23] T. Lundstrom and I. Rosenberg, J. Solid State Chem. **6**, 299 (1973).
[24] Y. Liang, W. Zhang, J. Zhao, and L. Chen, Phys. Rev. B **80**, 113401 (2009).
[25] D. M. Teter, MRS Bull. **23**, 22 (1998).
[26] Y. Liang and B. Zhang, Phys. Rev. B **76**, 132101 (2007).